Hindawi Publishing Corporation
Mathematical Problems in Engineering
Volume 2015, Article ID 462072, 8 pages
http://dx.doi.org/10.1155/2015/462072

Research Article

Optimal Lunar Landing Trajectory Design for Hybrid Engine

Dong-Hyun Cho,[1] Donghoon Kim,[2] and Henzeh Leeghim[3]

[1]*IT Convergence Technology Team, KARI, Daejeon 305-806, Republic of Korea*
[2]*Department of Aerospace Engineering, Texas A&M University, College Station, TX 77843-3141, USA*
[3]*Department of Aerospace Engineering, Chosun University, Gwangju 501-759, Republic of Korea*

Correspondence should be addressed to Henzeh Leeghim; h.leeghim@controla.re.kr

Received 15 January 2015; Revised 26 May 2015; Accepted 27 May 2015

Academic Editor: Gen Qi Xu

The lunar landing stage is usually divided into two parts: deorbit burn and powered descent phases. The optimal lunar landing problem is likely to be transformed to the trajectory design problem on the powered descent phase by using continuous thrusters. The optimal lunar landing trajectories in general have variety in shape, and the lunar lander frequently increases its altitude at the initial time to obtain enough time to reduce the horizontal velocity. Due to the increment in the altitude, the lunar lander requires more fuel for lunar landing missions. In this work, a hybrid engine for the lunar landing mission is introduced, and an optimal lunar landing strategy for the hybrid engine is suggested. For this approach, it is assumed that the lunar lander retrofired the impulsive thruster to reduce the horizontal velocity rapidly at the initiated time on the powered descent phase. Then, the lunar lander reduced the total velocity and altitude for the lunar landing by using the continuous thruster. In contradistinction to other formal optimal lunar landing problems, the initial horizontal velocity and mass are not fixed at the start time. The initial free optimal control theory is applied, and the optimal initial value and lunar landing trajectory are obtained by simulation studies.

1. Introduction

The lunar landing trajectory is a good example for the optimal problem because the dynamics is very simple, and the various energy-like values can be selected as a candidate for the cost function of the optimization problems. For these reasons, many researches have been focusing on designing the optimal lunar landing trajectory. In general, the lunar landing is divided into two phases: deorbit burn and powered descent phases. In the first phase, the lunar lander falls down to reduce the altitude from the lunar parking orbit. At this phase, the target perilune altitude is usually chosen between 10 km and 15 km from the lunar surface to avoid mountainous lunar terrain and potential guidance errors. For the deorbit burn maneuver, the Hohmann transfer method is widely applied by using impulsive thrusters. At the periapsis of the transfer orbit, the second phase is initiated to land on the lunar surface. The initial states of the powered descent phase can be in general calculated by the Hohmann transfer, and the continuous thruster is applied to reduce the ground speed on the second phase.

Most researches for the optimal lunar landing trajectory problem are focused on the powered descent phase by using a continuous thruster. To find an optimal solution, two-dimensional (2D) dynamics has been studied by many researchers because of their simplicity. Park et al. designed the optimal trajectory for the specific landing site by issuing a pseudospectral method in 2D space, and the solution is generally used for the optimal lunar landing researches [1]. Before this research, Ramanan and Lal suggested the same optimal lunar landing strategies and analyzed the strategies on a case-by-case basis for the various perilune altitudes [2]. In general, the lower perilune altitude saves fuel for the landing in the powered descent phase, but fuel for the deorbit burn is increased. Therefore, Ramanan and Lal also tried to find a suitable perilune altitude for whole lunar landing phases. Cho et al. suggested a similar approach for the initial free optimal problem, and the optimal perilune altitude is also designed with the optimal powered descent trajectory [3]. In addition to the research, there are many other approaches to find the optimal lunar landing trajectory. Shan and Duan also studied 2D lunar landing problems with

variable thrust level [4], and Hawkins solved a vertical lunar landing problem by using spacecraft rotational motions [5]. For the vertical lunar landing, Cho et al. also suggested an approach by using the path constraint [6]. Peng et al. applied the hybrid optimization algorithm for the optimal lunar landing trajectory design problem [7, 8]. In the guidance problem, Liu et al. studied the landing guidance control by using the optimal lunar landing trajectory [9, 10]. McInnes suggested another guidance strategy for a vertical landing by using the gravity-turn technique [11]. Zhou et al. studied a vertical lunar landing problem by using the attitude state variable [12].

In these optimal lunar landing trajectories, the lunar lander frequently increased its altitude to earn enough time to reduce the horizontal velocity. In this paper, an optimal solution is obtained for the hybrid engine. The hybrid engine means that the lunar lander has an impulsive and continuous thruster, and some researches have been performed for the orbit transfer by using this hybrid engine. The Hohmann Spiral Transfer (HST) is one of the examples [13, 14]. The authors assume that the lunar lander retrofired the impulsive thruster to reduce the horizontal velocity rapidly at the initiated time for the powered descent phase. Then, the lunar lander reduced the total velocity and altitude for the lunar landing by using the continuous thruster. By using this approach, the total mass consumption can be reduced. The authors tried to find the optimal retrofired velocity and trajectory to maximize the final landing mass. To solve this problem, the free initial problem for the impulsive thruster using the typical approach is considered.

2. Problem Definition

2.1. Assumptions. To derive the formula and perform the numerical simulation, the following assumptions are utilized.

(i) The gravity field of the moon is uniform through the whole path of the lunar lander, and the moon is entirely spherical. Therefore, one can easily apply the two-body dynamics to this problem.

(ii) The moon rotates on its own axis with the constant angular velocity. Moreover, the lunar parking orbit (circular orbit), the lunar landing trajectory, and the lunar equator are placed in the same plane, and each rotation direction is the same as well. Therefore, one can easily apply the 2D dynamics.

(iii) The initial trajectory of the lunar parking orbit is the circular orbit, and Hohmann transfer method is used for the deorbit burn phase. Therefore, the initial velocity of the powered descent phase can be calculated.

(iv) During the powered descent phase, the thrust of the lander is constant.

(v) There are no external perturbations.

2.2. Governing Equations. Using the above-mentioned assumptions, two-body and 2D dynamics are used. For these equations of motion, the polar coordinated system is selected as shown in Figure 1, and the governing equations for the lunar lander are described as follows [3]:

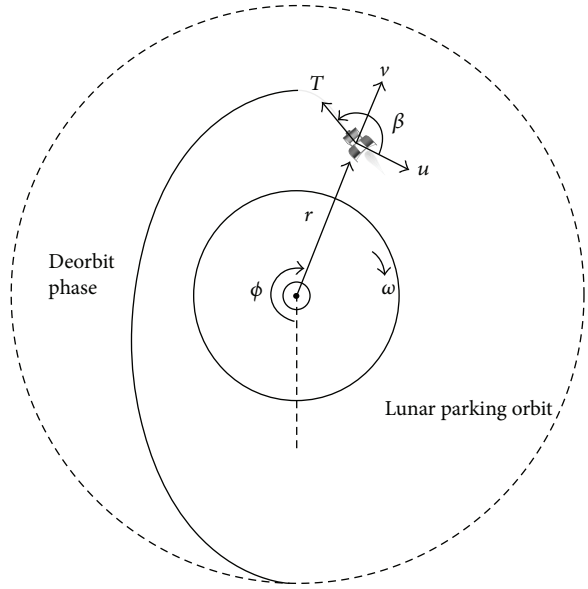

Figure 1: The polar coordinate system for the lunar lander.

$$\dot{r} = v, \tag{1}$$

$$\dot{\phi} = \frac{u}{r}, \tag{2}$$

$$\dot{u} = -\frac{uv}{r} + \frac{T}{m}\cos\beta, \tag{3}$$

$$\dot{v} = \frac{u^2}{r} - \frac{\mu}{r^2} + \frac{T}{m}\sin\beta, \tag{4}$$

$$\dot{m} = -\frac{T}{I_{sp}g}, \tag{5}$$

where r and ϕ are the radial distance and the position angle from the origin of the moon, u and v are the transverse and the radial velocity, m is the mass property of the lander, and μ is the standard gravitational parameter. The position angle is defined from the initial position of a deorbit burn phase. To describe the mass flow rate ($\dot{m}$), the specific impulse (I_{sp}) and the gravitational acceleration on the Earth (g) are adopted in (5). To express the thruster, T and β are used as a thrust magnitude and a thrust vector angle. The thrust vector angle is chosen to be a unique control input parameter during the powered descent phase.

2.3. Cost Function. It is intended to find the landing trajectory to minimize the fuel consumption by using the retrofired velocity at the initial time of the powered descent phase. Thus, the minimum fuel problem is equivalent to the maximum final landing mass problem. For this reason, the optimal landing trajectory to maximize the final landing mass is

designed, and the cost function for this problem is established as follows:

$$J = -m_f, \tag{6}$$

where m_f is the maximum final landing mass.

2.4. Boundary Conditions. Hohmann transfer method is used during the deorbit burn phase, and thus the initial horizontal velocity state of the powered descent phase is described as follows [15]:

$$V_0 = \sqrt{\mu\left(\frac{2}{r_0} - \frac{2}{r_0 + r_p}\right)}, \tag{7}$$

where r_p is the radial distance of the circular lunar parking orbit and the value is usually 100 km. Also, r_0 is the initial radial distance at the powered descent phase. In general, this altitude is the same as the perilune altitude of deorbit burn phase, and it is chosen between 10 km and 15 km due to mountainous lunar terrain and potential guidance errors. Here, the perilune altitude is assumed as 15 km from the lunar surface.

The impulsive thruster retrofired at the initial time of the powered descent phase. Therefore, the initial horizontal velocity (u_0) is not fixed and it is one of the optimal parameters. However, there is a relationship between the initial horizontal velocity and the initial mass from the rocket equation as follows [15]:

$$m_0 = M \exp\left(\frac{u_0 - V_0}{I_{\text{sp}} g}\right), \tag{8}$$

where M represents the initial total mass of the lunar lander.

In addition, the starting point of the deorbit burn phase is used as a reference point of the position angle (ϕ), and the perilune position is the opposite site from this reference position. Thus, the initial position angle is set as 180 degrees. Now, the initial states of the lunar lander at the initiated time of the powered descent phase can be described as follows:

$$\begin{aligned} r_0 &= 15 + r_{\text{moon}}, \\ \phi_0 &= 180^\circ, \\ u_0 &= \text{unkown}, \\ v_0 &= 0, \\ m_0 &= m \exp\left(\frac{u_0 - V_0}{I_{\text{sp}} g}\right), \end{aligned} \tag{9}$$

where r_{moon} is the radius of the moon.

For the lunar landing mission, the final radial distance must be the same radius of the moon, and horizontal and vertical velocities must be equal to the ground speed of the lunar surface. However, in this paper, the final position angle is not fixed because of the following assumptions: the moon is entirely spherical and the gravity field is uniform. Therefore, one can change the initial position of the deorbit burn phase to adjust the specific final position angle. Thus, the final position angle is not important. In addition, we want to find the optimal trajectory to maximize the final lunar mass, which is not fixed. For these reasons, the final state constraints are described as follows:

$$\begin{aligned} r_f &= r_{\text{moon}}, \\ \phi_f &= \text{free}, \\ u_f &= r_{\text{moon}}\omega, \\ v_f &= 0, \\ m_f &= \text{free}, \end{aligned} \tag{10}$$

where the subscript f means the value at the final landing time and ω represents the rotation velocity of the moon.

3. Optimal Trajectory Design

3.1. Optimal Theory. To solve the defined optimal problem, the indirect method based on the calculus variation is used because of simple system dynamics. The Hamiltonian function is established from the system dynamics and cost function in the previous section as follows:

$$H = \lambda_r \dot{r} + \lambda_\phi \dot{\phi} + \lambda_u \dot{u} + \lambda_v \dot{v} + \lambda_m \dot{m}, \tag{11}$$

where λ_r, λ_ϕ, λ_u, λ_v, and λ_m represent the costate variables for each state variable and the subscripts indicate the state variables. From the optimal control theory, the dynamics of costates can be obtained as follows [16]:

$$\dot{\lambda} = -H_x^T. \tag{12}$$

Therefore, the similar equations of each costate to the other researches can be formulated as follows:

$$\begin{aligned} \dot{\lambda}_r &= \lambda_\phi \frac{u}{r^2} - \lambda_u \frac{uv}{r^2} + \lambda_v \left(\frac{u^2}{r^2} - 2\frac{\mu}{r^3}\right), \\ \dot{\lambda}_\phi &= 0, \\ \dot{\lambda}_u &= -\frac{\lambda_\phi}{r} + \lambda_u \frac{v}{r} - \lambda_v \frac{2u}{r}, \\ \dot{\lambda}_v &= -\lambda_r + \lambda_u \frac{u}{r}, \\ \dot{\lambda}_m &= \frac{T}{m^2}\left(\lambda_u \cos\beta + \lambda_v \sin\beta\right). \end{aligned} \tag{13}$$

Then, the control command can also be obtained from the optimal control theory. The control variable must satisfy the following two equations to minimize the cost function:

$$\begin{aligned} \frac{\partial H}{\partial \beta} &= -\frac{T}{m}\left(\lambda_u \sin\beta - \lambda_v \cos\beta\right) = 0, \\ \frac{\partial^2 H}{\partial \beta^2} &= -\frac{T}{m}\left(\lambda_u \cos\beta + \lambda_v \sin\beta\right) > 0. \end{aligned} \tag{14}$$

The control command is generated as a function of the costates from (14) as follows:

$$\beta = \tan^{-1}\left(\frac{-\lambda_v}{-\lambda_u}\right). \tag{15}$$

Let us find the initial values of the costates satisfying the boundary conditions to design the optimal lunar landing trajectory. In the previous section, the boundary conditions of states were introduced. Also, the boundary conditions of the costates can be obtained from the optimal control theory.

Therefore, the augmented constraint function is written as follows:

$$G = \underbrace{-m_f}_{\text{Perfomance}} + \nu^T \underbrace{\psi\left(t_f, x_f\right)}_{\substack{\text{Final State}\\ \text{Constraints}}} + \xi^T \underbrace{\sigma\left(t_0, x_0\right)}_{\substack{\text{Initial State}\\ \text{Constraints}}}, \tag{16}$$

where the final and initial state constraints matrices are described as follows:

$$\psi = \begin{bmatrix} r_f - r_{\text{moon}} & u_f - r_{\text{moon}}\omega & v_f \end{bmatrix}^T,$$
$$\sigma = \begin{bmatrix} r_0 - \left(15 + r_{\text{moon}}\right) \\ \phi_0 - 180^\circ \\ v_0 \\ m_0 - M\exp\left(\dfrac{u_0 - V_0}{I_{\text{sp}}g}\right) \end{bmatrix}. \tag{17}$$

Contrary to the formal optimal lunar landing problem, this augmented constraint function has the term for the initial state constraints in (16). Due to this additional term, the boundary conditions of the costates and the Hamiltonian can be obtained from optimal theory [16]:

$$\begin{aligned} H_f &= -G_{t_f}, \\ \lambda_f &= G_{x_f}^T, \\ \lambda_0 &= -G_{x_0}^T. \end{aligned} \tag{18}$$

Using these equations, the boundary conditions of the costates and Hamiltonian are obtained as follows:

$$\begin{aligned} H_f &= 0, \\ \lambda_\phi\left(t_f\right) &= 0, \\ \lambda_m\left(t_f\right) &= -1, \\ \lambda_u(0) + \lambda_m(0)\frac{M}{I_{\text{sp}}g}\exp\left(\frac{u_0 - V_0}{I_{\text{sp}}g}\right) &= 0. \end{aligned} \tag{19}$$

Now, the initial costate values and initial horizontal velocity to satisfy these boundary conditions need to be found from (10), (18), and (19).

3.2. Solution of Two-Point Boundary Value Problem: Shooting Method. In the previous section, the optimal conditions based on the indirect method are evaluated. This optimal control problem can be reformulated to the two-point boundary value problem. Also, it is usually solved by using parameter optimization methods such as the sequential quadratic programming, evolutionary algorithm, genetic algorithm, coevolutionary augmented Lagrangian method, and particle swarm optimization. In general, these optimal solvers are divided into two categories: line search process and stochastic process. It is usually difficult to select a suitable search boundary of the solution in stochastic process. Therefore, the shooting method is applied to find the optimal solution.

For the shooting method, the constraints matrix (h) must be described at first. From the previous section, the constraints matrix is written as follows:

$$h = \begin{bmatrix} \lambda_u(0) + \lambda_m(0)\dfrac{M}{I_{\text{sp}}g}\exp\left(\dfrac{u_0 - V_0}{I_{\text{sp}}g}\right) \\ r_f - r_{\text{moon}} \\ u_f - r_{\text{moon}}\omega \\ v_f \\ \lambda_\phi\left(t_f\right) \\ \lambda_m\left(t_f\right) + 1 \\ H_f \end{bmatrix}. \tag{20}$$

Note that the constraint matrix is not a full matrix. For simplicity, the constraint matrix is described as the reduced form. The derivative of the constraint matrix is written as follows:

$$dh = \dot{h}_f dt_f + h_{z_0}\delta z_0 + h_{z_f}\delta z_f + \text{H.O.T}, \tag{21}$$

where $z = \begin{bmatrix} x^T & \lambda^T \end{bmatrix}^T$ represents the augmented state matrix and t_f represents the final time. Also, the subscripts 0 and f mean the values at the initial and final times. Here, the high order term is neglected, and the equation is rewritten for only the initial augmented state matrix and final time by using the state transition matrix (Φ):

$$dh = \begin{bmatrix} \dot{h}_f & h_{z_0} + h_{z_f}\Phi_f \end{bmatrix}\begin{bmatrix} dt_f \\ \delta z_0 \end{bmatrix}. \tag{22}$$

To reduce the constraints, one can choose the derivative of this constraints matrix as follows:

$$dh = -\alpha h, \quad 0 < \alpha \le 1. \tag{23}$$

From (22) and (23), the update law of the augmented state variables at the initial time is obtained as follows:

$$\begin{bmatrix} dt_f \\ \delta z_0 \end{bmatrix} = -\alpha\begin{bmatrix} \dot{h}_f & h_{z_0} + h_{z_f}\Phi_f \end{bmatrix}^{-1} h. \tag{24}$$

Using the update law, the optimal solution can be found by using an iterative process:

(i) Initially guess augmented state vector (z) and total fight time (t_f).

(ii) Propagate the system and costates dynamics (Equations ((1)–(5)) and (13)) with the optimal control law (Equation (15)) for the total flight time (t_f).

(iii) Calculate the constraint matrix and check it.

(A) If $\|h\|$ is less than tolerance value, then this shooting method terminates (the solution is obtained).

(B) If $\|h\|$ is not less than tolerance value, then calculate the updated value from (24) and add this value to the initial guessing value. Then, go to (ii) phase with these updated values.

4. Simulation

In the previous optimal lunar landing trajectories, the lunar lander frequently increased its altitude to earn enough time to reduce the horizontal velocity as shown in Figure 2 [1, 2]. This phenomenon depends on its thrust-mass ratio. For enough thrust, this increase in the altitude is reduced due to enough thrust. This phenomenon is plotted in the Figure 3. However, this huge thrust-mass ratio is sometimes not physically possible because of the cost, mass budget, thruster technology, and so forth. Thus, if the horizontal velocity at the initial time is reduced rapidly, it is possible to save fuel.

Using the derived conditions in the previous section, the proposed optimal approach is demonstrated based on the identical simulation conditions in [2]. For numerical simulations, it is assumed that lunar parking orbit is the circular orbit in the 100 km altitude. From this parking orbit, the lunar lander falls down to 15 km altitude by using Hohmann transfer method during the deorbit burn phase. Thus, the horizontal velocity before the retrofiring maneuver is calculated using (7) as follows:

$$V_0 = 1691.96926\ \text{m/s}. \tag{25}$$

The initial mass of lunar lander is set to 300 kg, and the constant thrust level and specific impulse of the thruster are also set to 440 N and 310 s to calculate the mass flow rate.

Under the simulation conditions, the optimal delta velocity of initial retrofiring maneuver and the optimal lunar landing trajectory are found by using the shooting method. The final landing mass of the previous and suggested optimal solution is listed in Table 1. Note that the suggested optimal solution saves about 6 kg fuel during the lunar landing phase in this case, and the saved fuel is about 4% of the total consumed fuel. From the numerical simulation, the required retrofiring velocity is obtained as follows:

$$\Delta V = 1200.9011\ \text{m/s}. \tag{26}$$

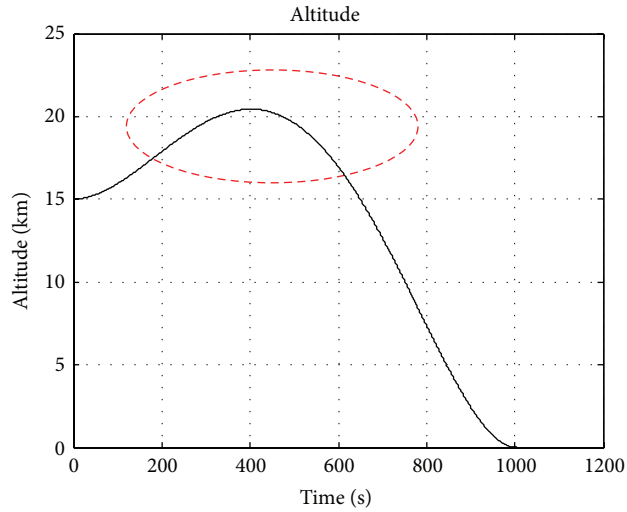

Figure 2: The typical optimal lunar landing trajectory [1].

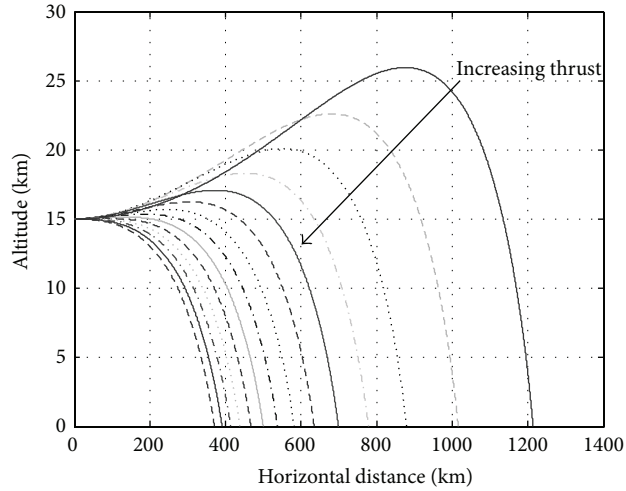

Figure 3: The optimal lunar landing trajectory for the ratio of thrust mass.

Table 1: Final landing mass.

	Final mass (kg)	Total fuel consumption (kg)
Previous optimal solution	154.5413	145.4587
Proposed optimal solution	160.6186	139.3814

Note that this value depends on the thrust-mass ratio for the other case and is also easily obtained by using the suggested approach. Due to this retrofiring maneuver, the lunar lander does not increase its altitude to earn enough time to reduce the horizontal velocity anymore, and this result is verified by plotting the lunar landing trajectory shown in Figure 4. In this figure, there is no more increase of altitude in comparison with the previous approach shown in Figure 2. Also, the horizontal velocity can be rapidly reduced, and the total flight time is also reduced to a third of the previous flight time. These horizontal and vertical velocity results are

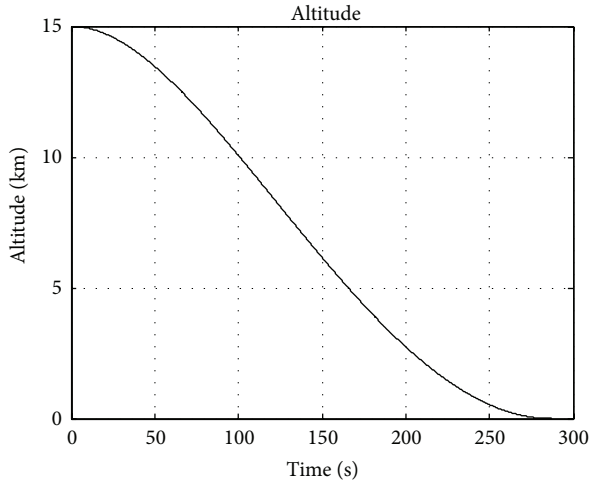

Figure 4: The altitude time history for the optimal solution.

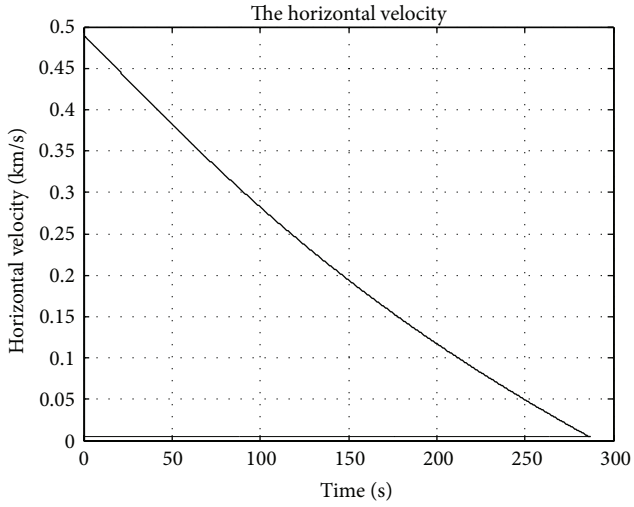

Figure 5: The horizontal velocity profile.

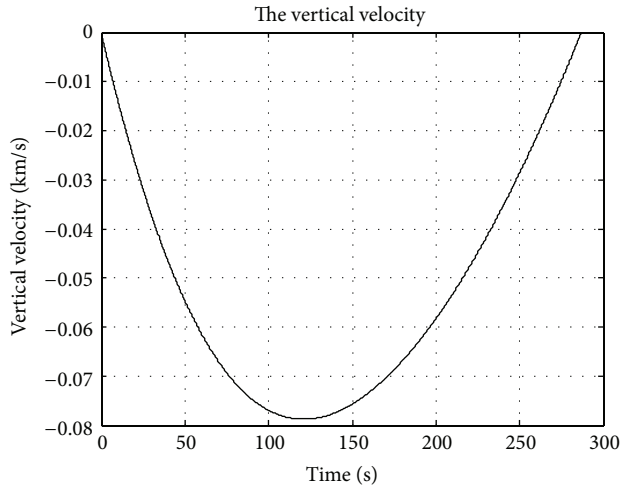

Figure 6: The vertical velocity history.

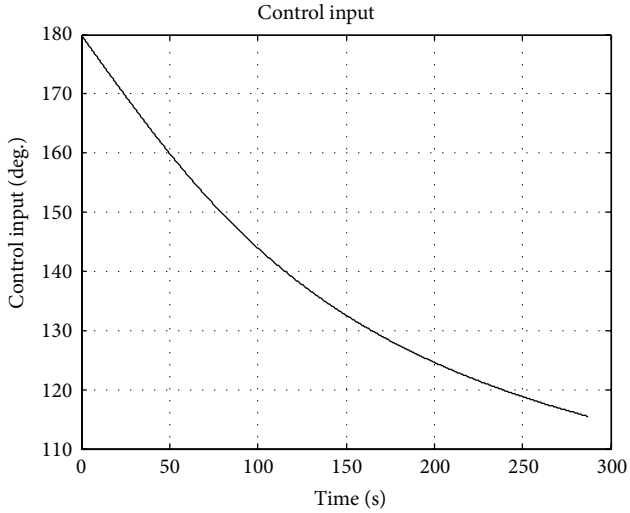

Figure 7: The control command for the optimal lunar landing.

plotted in Figures 5 and 6, respectively. In the vertical velocity plot, the vertical velocity is always negative, and there are no sign changes by comparing with the previous result. This also means that the altitude does not increase during the whole path. There are no sign changes in the vertical velocity, and the control command does not exceed 180 degrees as shown in Figure 7.

To check the optimality of this simulation result, the trend analysis is also demonstrated in Figure 8. This result can be obtained by applying the previous typical optimal lunar landing approach in [1, 2] by changing the initial delta velocity from 0 to 1,600 m/s with 50 m/s step. In this figure, the final landing mass is increasing as increasing the initial delta velocity, and this final landing mass is maximized near 1200 m/s. This value is similar to the optimal result using the suggested approach.

In this section, the simple optimal lunar landing problem by using the suggested method is demonstrated, and the optimal initial delta velocity with optimal lunar landing

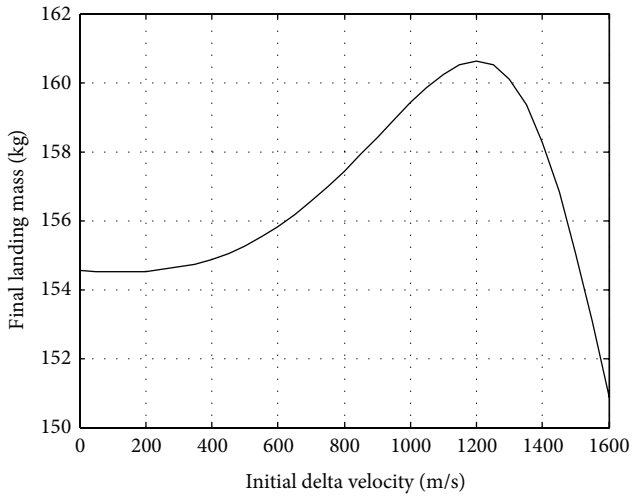

Figure 8: The final landing mass for the various retrofired velocity at the initiated time of the powered descent phase.

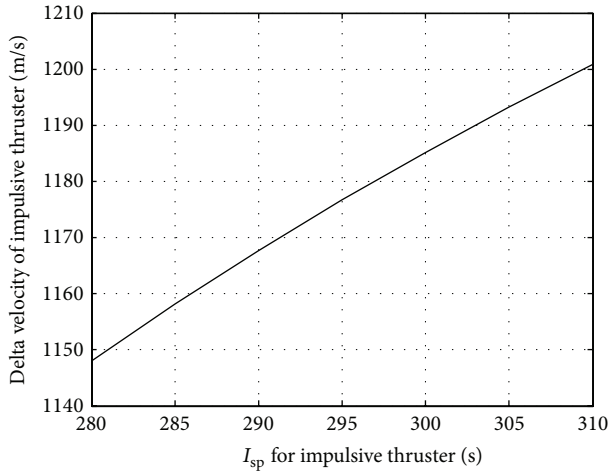

Figure 9: The optimal initial retrofired velocity for the specific impulse.

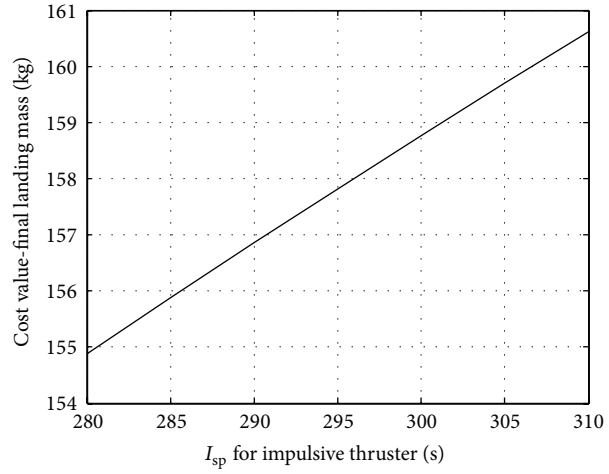

Figure 10: The optimal final landing mass for the specific impulse.

trajectory is obtained. However, this result depends on the specific impulse of the impulsive thruster. If the impulsive thruster has a low specific impulse, the mass consumption for the impulsive thruster is quietly increased more than the reduced fuel for the continuous thruster. To check this phenomenon, the simple trend analysis between the specific impulse of impulsive thruster and the optimal initial delta velocity is demonstrated in Figure 9. Actually, the specific impulse of impulsive thruster does not exceed the continuous thruster. Thus, in this figure, the specific impulse stepped down from 310 s which is the specific impulse of the continuous thruster, and the same suggested optimal approach is applied iteratively to obtain the optimal initial delta velocity. In this figure, the initial delta velocity is also decreased as decreasing the specific impulse of impulsive thruster because of the low efficiency of impulsive thruster. For this trend analysis, the final lunar landing mass can be obtained by using suggested optimal approach and it can be depicted in Figure 10. In this figure, the final landing mass is decreased as decreasing the specific impulse of impulsive thruster. If the specific impulse of impulsive thruster less than 280 sec is supposed to be selected for this case, it does not provide any benefit for the final lunar landing mass.

5. Conclusions

An optimal lunar landing strategy by using the hybrid engine is suggested in this paper. The typical optimal lunar landing trajectory sometimes requires the increase in altitude to earn the time to reduce the horizontal velocity. This increase in altitude is not efficient for the maximization of the final landing mass. To reduce the horizontal velocity rapidly, the retrofiring maneuver is applied at the initial time of the powered descent phase by using the impulsive thruster. The initial state free optimization theory is applied, and the suitable and more efficient solution is obtained. As a result, it is discovered that the lunar lander has more capability to carry out the mission. To conclude, one can makes various lunar landing problems and also obtain various solutions by using the initial state free optimization approach.

Conflict of Interests

The authors declare that there is no conflict of interests regarding the publication of this paper.

Acknowledgments

This research was supported by the project "A Development of Core Technology for Space Exploration Using Nano-satellite" funded by the Korea Aerospace Research Institute (KARI). The authors would like to thank KARI for their support.

References

[1] B.-G. Park, J.-S. Ahn, and M.-J. Tahk, "Two-dimensional trajectory optimization for soft lunar landing considering a landing site," *International Journal of Aeronautical & Space Sciences*, vol. 12, no. 3, pp. 288–295, 2011.

[2] R. V. Ramanan and M. Lal, "Analysis of optimal strategies for soft landing on the moon from lunar parking orbits," *Journal of Earth System Science*, vol. 114, no. 6, pp. 807–813, 2005.

[3] D. H. Cho, B. Jeong, D. Lee, and H. Bang, "Optimal perilune altitude of lunar landing trajectory," *International Journal of Aeronautical and Space Sciences*, vol. 10, no. 1, pp. 67–74, 2009.

[4] Y. Shan and G. Duan, "Study on the optimal fuel consumption of the singularity condition for lunar soft landing," in *Proceedings of the IEEE International Conference on Robotics and Biomimetics (ROBIO' 07)*, pp. 930–935, December 2007.

[5] A. M. Hawkins, *Constrained trajectory optimization of a soft lunar landing from a parking orbit [Thesis]*, MIT, 2005.

[6] D.-H. Cho, H. Bang, and H.-D. Kim, "Optimal trajectory design for the lunar vertical landing," in *Proceedings of the 63rd International Astronautical Congress (IAC '12)*, pp. 5662–5669, October 2012.

[7] Q.-B. Peng, H.-Y. Li, H.-X. Shen, and G.-J. Tang, "Hybrid optimization of powered descent trajectory for manned lunar mission," *Transactions of the Japan Society for Aeronautical and Space Sciences*, vol. 56, no. 3, pp. 113–120, 2013.

[8] Q. Peng, "Finite-thrust trajectory optimization using a combination of gauss pseudospectral method and genetic algorithm," in *Genetic Algorithms in Applications*, chapter 4, InTech, Rijeka, Croatia, 2012.

[9] X. Liu and G. Duan, "Nonlinear optimal control for the soft landing of lunar lander," in *Proceedings of the 1st International Symposium on Systems and Control in Aerospace and Astronautics (ISSCAA '06)*, pp. 1381–1387, Harbin, China, January 2006.

[10] X.-L. Liu, G.-R. Duan, and K.-L. Teo, "Optimal soft landing control for moon lander," *Automatica*, vol. 44, no. 4, pp. 1097–1103, 2008.

[11] C. R. McInnes, "Path shaping guidance for terminal lunar descent," *Acta Astronautica*, vol. 36, no. 7, pp. 367–377, 1995.

[12] J. Y. Zhou, K. L. Teo, D. Zhou, and G. H. Zhao, "Optimal guidance for lunar module soft landing," *Nonlinear Dynamics and Systems Theory*, vol. 10, no. 2, pp. 189–201, 2010.

[13] S. Owens and M. MacDonald, "Analogy to bi-elliptic transfers incorporating high- and low-thrust," *Journal of Guidance, Control, and Dynamics*, vol. 36, no. 3, pp. 892–895, 2013.

[14] S. Owens and M. MacDonald, "An extension and numerical analysis of the hohmann spiral transfer," in *Proceedings of the 63rd International Astronautical Congress (IAC '12)*, pp. 5628–5639, October 2012.

[15] V. A. Chobotov, *Orbital Mechanics*, AIAA Education Series, 1996.

[16] D. G. Hull, *Optimal Control Theory for Applications*, Mechanical Engineering Series, Springer, New York, NY, USA, 2003.